SEMARAK ILMU PUBLISHING

CFD Letters

Journal homepage:
https://semarakilmu.com.my/journals/index.php/CFD_Letters/index
ISSN: 2180-1363

CFD Analysis of the Effect of Heat Distribution on Different Heating Pad Piping Arrangements for Flexitank Application

Syafiqah Ruqaiyah Saiful Azam[1], Nofrizalidris Darlis[2,*], Norrizal Mustaffa[1], Mohamad Amirur Rahman Azahar[1], Amirul Syafiq Bin Sadun[3], Omar Abu Hassan[3], Ishkrizat Taib[4], Khairul Nizam Mustaffa[5], Muhamad Mohshein Hashim[5]

[1] Department of Mechanical Engineering Technology, Faculty of Engineering Technology, Universiti Tun Hussein Onn Malaysia, Pagoh Education Hub, Pagoh, Johor, Malaysia
[2] Integrated Engineering Simulation and Design, Faculty of Engineering Technology, Universiti Tun Hussein Onn Malaysia, Pagoh Education Hub, Pagoh, Johor, Malaysia
[3] Department of Electrical Engineering Technology, Faculty of Engineering Technology, Universiti Tun Hussein Onn Malaysia, Pagoh Education Hub, Pagoh, Johor, Malaysia
[4] Faculty of Mechanical and Manufacturing Engineering, Universiti Tun Hussein Onn Malaysia (UTHM), Batu Pahat, Johor, Malaysia
[5] My Flexitank Industries Sdn Bhd, Plot 3&4, Jalan PKNK 3, Kawasan Perindustrian LPK Fasa 3, 08000 Sungai Petani, Kedah, Malaysia

ARTICLE INFO

Article history:
Received 11 August 2022
Received in revised form 12 September 2022
Accepted 10 October 2022
Available online 1 February 2023

Keywords:
Floor Heating system; Temperature Distribution; Underfloor Heating Design; Heat Transfer; Computational Fluid Dynamics (CFD)

ABSTRACT

Variations in piping arrangements of heating pad for flexitank applications causes a difference in the time required to completely liquidise the liquid during the discharging process. As reference, a conventional heating pad took about 48 hours to heat up the flexitank. There are many commercials heating pad used in flexitank applications to facilitate the discharging process of liquid. However, there are still uncertainty or limitation reference regarding the heating pad for flexitank application. One of the solutions to minimize the time taken for discharging process is identify the finest piping arrangement of heating pad. Based on the previous study, piping arrangement plays an important role for performance of the heating pad heat distribution. Thus, this paper aims to study the thermal behaviour of different heating pad arrangement for flexitank application with references to commercial arrangement of floor heating pad based on various inlet pressure using computational fluid dynamics (CFD) simulation software. This study was done by comparing thermal analysis of three piping arrangement which is conventional arrangement, Serpentine arrangement, and Spiral arrangement. The geometry of heating pad was created using Computer-Aided Design (CAD) software, SolidWorks. The results have discussed some important components parameter that must be controlled for the system to function efficiently. These parameters include pressure distribution within the pipes, temperature distribution along the pipes, and piping arrangement patterns. The simulation results show that the Counterflow arrangement has a uniform temperature distribution between the inlet and outlet. The study concluded that counterflow arrangement generally the best arrangement among these three since the configuration allowing less pressure losses and better thermal distribution on flexitank and heating pad. This study is therefore useful for designers to explore more adequately the benefits of underfloor heating system on many applications.

* *Corresponding author.*
E-mail address: nofrizal@uthm.edu.my (Nofrizalidris Darlis)

https://doi.org/10.37934/cfdl.15.2.115

1. Introduction

Flexitank are a versatile tool for transporting bulk liquid. However, some liquids that have a higher viscosity or solidify are more difficult to discharge after becoming (cold) during transit to cold weather areas. When this circumstance occurred, the heating pad is required since its function is to uniformly reheat the entire space below the flexitank to allow the maximum exposure to completely reheat the product [1]. Frequently in the commercial market, majority company are used steam, hot water and electric as their heat source. The maximum temperature used is 124 C and the maximum pressure used was 20 bars in spite of that, the majority of companies only utilize 1 to 4 bars. The material used for commercial heating pad are ethylene propylene diene monomer (EPDM), rubber, aluminium film, metal, caoutchouc, and polyethylene (PE) [2–6].

According to the reported cases from company that produce conventional heating pad, it took more than 48 hours to completely reheat the flexitank [3]. There are many commercials heating pad used in flexitank applications to facilitate the discharging process of liquid. However, there are still uncertainty or limitation reference regarding the heating pad for flexitank application. The most of previous research was conducted on floor heating pads, with applications similar to heating pads for flexitank [7–13]. One of the solutions to minimize the time taken to completely liquidize for discharging process is identify the finest arrangement of heating pad.

There are numerous studied focused on the piping arrangement of the heating pad, this indicates that arrangement plays a vital impact on the enhancement of the heat dissipation. Oubenmoh *et al.,* [14] conducted a numerical simulation on three different piping arrangements which are Serpentine, Counterflow and Modulated spiral arrangement. The simulation results revealed that the heat distribution of spiral arrangement was the best arrangement since its configuration allowed less pressure losses and better thermal homogenization.

Mishra *et al.,* [9] used an academic version of the commercial CFD code ANSYS Fluent to compare temperature distribution in the floor cross section and floor surface of two different piping layouts. According to Mishra *et al.,* [9] analysis's the counterflow spiral type arrangement is the optimum option for creating uniform temperature distribution in the floor surface where the application is similar to the heating pad for flexitank applications.

In summary, the majority of previous numerical studies focused on the arrangement for a floor heating pad even on building application on flexitank applications. CFD approach is frequently used by researchers in study the thermal behavior of the heating system. Due to the high cost in preparation of the actual heating pad arrangement and maintenance, it is suggested to use numerical approach to predict the thermal performance of a heating system. The objective of this study is to study the thermal behavior of different heating pad arrangement for flexitank application with references to commercial arrangement of floor heating pad based on various inlet pressure using CFD software. The simulation results are carried out to assess particularly temperature distribution on the tubing surface and flexitank surface. Furthermore, pressure losses for three tubing forms are assessed. This research will help designers better understand the benefits of an underfloor heating system in a variety of applications.

2. Methodology

2.1 Geometry Modeling

A heating pad and flexitank 21,000 L model geometry was created using SolidWorks 2021 computer aided design software, which was then combined into Ansys 19.2 for numerical calculation. A model geometry of flexitank were generated for the simulation of show the efficiency of heat

distribution on the heating pad when apply to flexitank. The details on the geometry of the actual design will be discussed in this section.

The geometry model of heating pad arrangement was built with the reference from the commercial heating pad in the market and also arrangement of floor heating pad for building application as shown in Table 1. The conventional heating pad system was constructed completely in accordance with the dimensions and specifications specified by the company My Flexitank Sdn Bhd, whereas the spiral and counterflow arrangements were constructed in accordance with previous floor heating pad research conducted by Oubenmoh *et al.,* [14] and Aacharya *et al.,* [12] as shown in Figure 1.

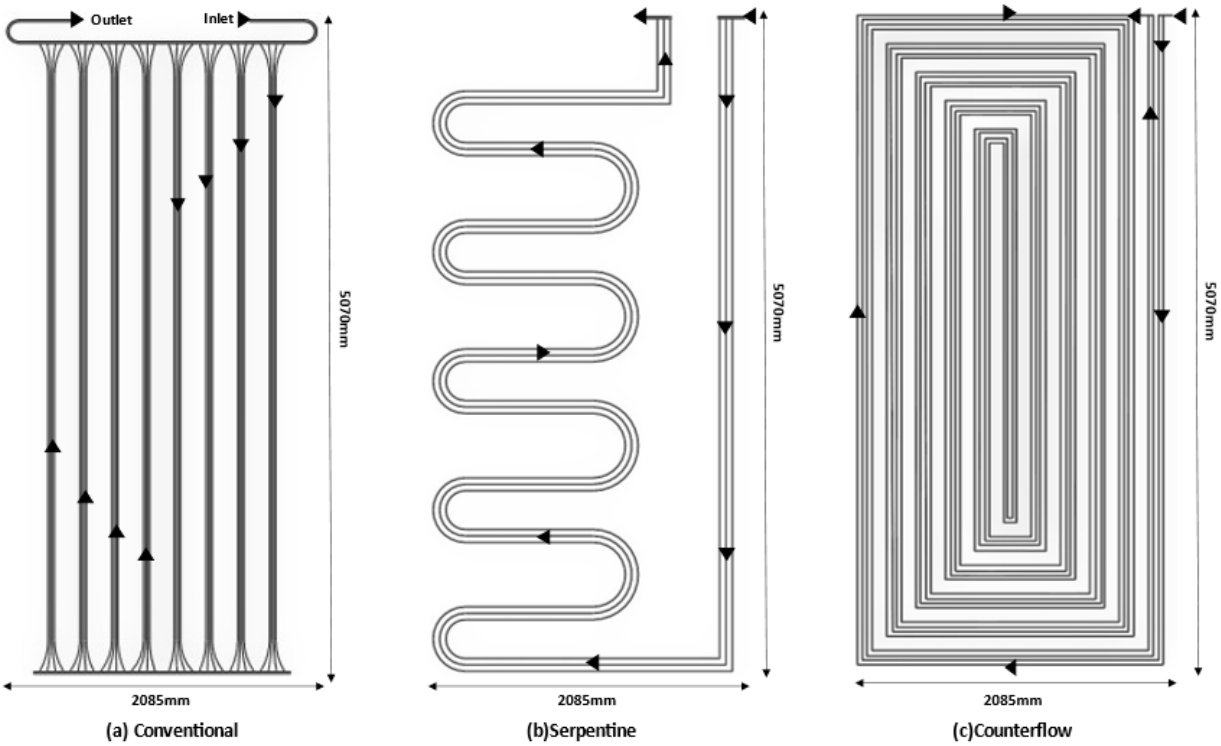

Fig. 1. Configuration of heating pad with different piping arrangement; (a) Conventional arrangement [3], (b) Serpentine [14] and (c) Counterflow [12] arrangement

Table 1
Geometric parameters of the heating pad

Parameter		Dimension (mm)
Layout (L x W)		5070 x 2085
Diameter	Inner	6
	Outer	10
Material		Ethylene Propylene Diene Monomer (EPDM) rubber

2.2 Mesh Study

The 3-dimensional fluid domain geometry of heating pad and flexitank had been imported from SolidWorks and the mesh of control volume is generated in ANSYS CFX 19.2 [15] as shown in Figure 2.

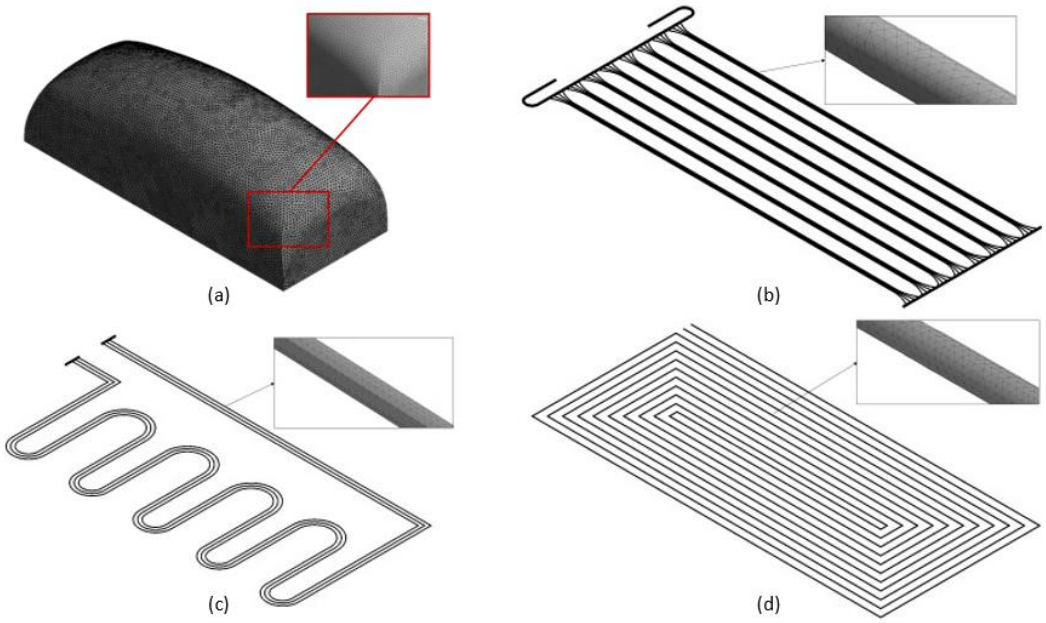

Fig. 2. Mesh generation for (a) Flexitank, (b) Conventional arrangement, (c) Serpentine and (d) Counterflow arrangement

Due to the complex geometry, the heating pad attached to the simplified model was meshed with tetrahedral mesh. Due to the unsymmetrical and complex geometry, the tetrahedral mesh was set for all sections of the heating pad attached to the simplified geometry of flexitank at patient-specific model. The mesh statistics for different mesh refinements is shown in Table 2.

Table 2
Mesh statistics for different mesh refinements

Case	Case A	Case B	Case C
Number of elements	5379524	2085654	1667498
Number of nodes	1764243	701666	672909

Grid independent tests with mesh size and number of nodes meshes had been performed on the heating pad model to minimize the error due to discretization, and the average error in velocities was set to less than 1%. Because it is the most complex and main geometry for this numerical simulation, the heating pad model was chosen for this test [16, 17].

2.3 Numerical Procedure

2.3.1 Fluid flow characteristics and simulation assumptions

In this study, heating pads was simulated for the pipe section using Computational Fluid Dynamics and compared the results in terms of temperature distribution for different piping arrangements. Layout of the heating pad was constructed for 5070mm, length x 2085mm, width. The pipe shaping and the piping arrangement significantly impacts heat output, thermal performance, and temperature distribution of the flexitank. The model included the three different piping arrangements, having a pipe outer diameter of 10 mm and inner was 6mm. Three piping layouts, namely conventional heating pad, serpentine arrangement, and counterflow arrangement as shown in Figure 1. The following assumptions underpin the numerical simulation of these heating pad systems:

i. Steam was used as a working fluid.
ii. The fluid is considered as incompressible and uniform.
iii. The fluid has constant pressure inlet.
iv. Around the pipes was considered as adiabatic walls [18, 19].
v. Steady-state condition has been considered.

2.3.2 Governing equations

An algebraic equation is discretised using the pressure-based finite volume method before being numerically solved. The velocity and temperature field solutions are generated using different convergence criteria. In the wall boundary condition, a 'couple' wall is used to allow conjugate heat transfer between the solid-fluid interface. A geometric model is separated into two domains for this purpose: tube pipes as a solid domain and working fluid as a fluid domain. To solve and evaluate the laminar flow in the absorber tube, the viscous laminar model is selected. Based on the assumptions stated above, the fluid flow through the heating pad system is incompressible and steady. The governing equations of continuity, momentum, and flow energy are shown below if the heating pad system is considered as a control volume [20-22].

Continuity equation:

$$\nabla \cdot \left(\rho_{nf} \vec{V}_{nf}\right) = 0 \tag{1}$$

Momentum equation:

$$\nabla \cdot \left(\rho_{nf} \vec{V}_{nf} \vec{V}_{nf}\right) = -\nabla \mathrm{P} + \nabla\left(\mu_{nf} \nabla \vec{V}_{nf}\right) \tag{2}$$

Flow energy equation:

$$\nabla \cdot \left(\vec{V}_{nf} \rho_{nf} C_{p.nf} T_{nf}\right) = -\nabla P + \nabla(k_{nf} \nabla T_{nf}) \tag{3}$$

In the equation above, $\vec{V}_{\mathrm{nf}}$, P, ρ_{nf}, μ_{nf}, $C_{\mathrm{p,nf}}$, T_{nf}, k_{nf} are fluid velocity, pressure, density, shear stress, specific heat capacity, temperature, and thermal conductivity. The subscript nf refers to the nanofluid used in the study.

2.3.3 Numerical setup

In this study, three different piping arrangements, conventional arrangement, serpentine and counterflow arrangements with the same layout dimension and diameter tube were used with constant pressure inlet of steam. The simulations were carried out with the Academic release of ANSYS code CFX, a CFD analysis software programme. It employs the Finite Volume Method (FVM) to solve the Particle Equation Differential numerically (PDEs) [9, 12, 14]. The governing equations include the Navier-Stokes equation, as well as the laws of conservation of mass, momentum, and energy. The convergence residuals are maintained as the default value, and the iteration ends when the residual values of energy, continuity, and energy meet the specified value. The RNG k-ε turbulence model was used to simulate. The k-ε model is a two-equation model in which k is the turbulent kinetic energy transport equation and is the ε eddy dissipation equation [23]. The energy

equation was also solved in order to describe the thermal energy exchange between the fluid flow and the solid domain. The numerical simulation applied 'pressure inlet' to the working fluid inlet. The 'inlet' temperature was kept constant dependent on the temperature of the steam. Because the fluid is incompressible, the 'pressure outlet' boundary condition is chosen for the working fluid's outflow. A 'no slip' boundary condition is also applied to the walls at the boundary condition. The lateral surrounding wall of the pipes is considered to be adiabatic. Summary of the boundary conditions is shown in Table 3.

Table 3
Boundary conditions

Boundary Conditions		Case A	Case B	Case C
Inlet pressure	Pressure (bar)	1-4	1-4	1-4
	Temperature °C	100	100	100
Outlet pressure (bar)		0	0	0
Wall		Non-slip condition	Non-slip condition	Non-slip condition

3. Verification and Validation

In order to verify and validate the geometry of the heating pad, simulation of the 3-dimensional steady state approach was conducted in the CFD software in order to predict the average pipe surface temperature and the effectiveness of the configuration. By comparing experimental and numerical data, the verification and validation stage is achieved.

3.1 Experimental Setup

Heating pad used in this study is shown in Figure 3. It comprised of 32 flow tubes which are consist of 16 tubes for inlet flow while other 16 was the outlet flow with the inner diameter 6mm and the outer diameter was 10mm. Then, the main entry inlet and outlet manifold of the heating pad were designed with outer diameter 25.4 mm with thickness 4.2mm. The material used for the 32 tubes flow is EPDM rubber while the main entry inlet and outlet used stainless steel for the material. The dimension of the heating pad was in millimeters, 5070mm for a length and the width was 2085mm.

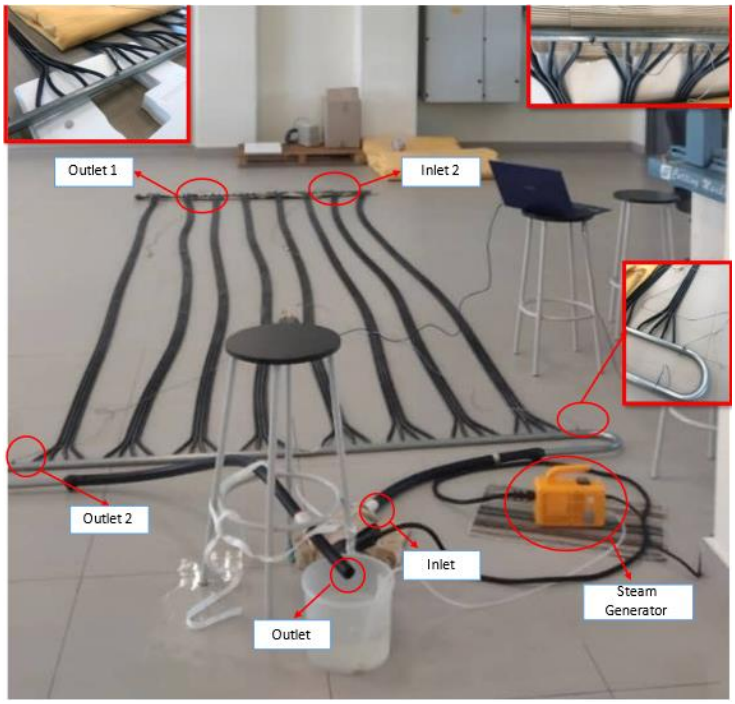

Fig. 3. Experimental setup

As illustrated in Figure 4, the temperature at the heating pad was measured by attaching the temperature sensor at various points using thermocouple type K. Thermocouples consist of two wires, of different types of metal, that are joined together in the end. This junction is where the temperature is measured (the cable tip). When the junction is heated, a voltage is created, and this can be used to calculate the temperature inside the stainless steel. Figure 4 shows the thermocouple that had been used for this experimental study. Data collection for four points was collected using data logger (Pico Technology USB TC-08 Thermocouple Temperature data Logger with K Sensor) since Data loggers are electronic devices that continuously monitor and record environmental parameters. Conditions can be monitored, documented, analysed, and validated using data loggers. The data is collected by a sensor and stored in the data logger by a computer chip. The information from the data logger is subsequently sent to a computer for analysis. Figure 4 shows the data logger used to collect the data. Through this technique, it was assumed that the motion of the steam exactly flows and heat up the heating pad, since the temperature reading can be collected within a time its travel and heat up the sensor point.

Fig. 4. Thermocouple sensor and data logger

4. Result and Discussion

4.1 Grid Independence Test

The term grid independence test describes the idea of improving calculation results of a calculation by using successively smaller cell sizes for the calculation. The mesh should approach similar results as the cell size gets smaller, hence the term of grid independence test [19, 20]. A mesh independency test is performed to determine how the simulation results are affected by mesh density [24]. In order to achieve mesh independence, the geometry model's mesh size is further refined to produce much more cells thus the accuracy of the numerical calculation will more accurate.

The element and node numbers with varying element sizing shown in Table 2 were used for the current study since further mesh refinement has no significant influence on the study. Figure 5 illustrates the velocity distribution of a heating pad design with varying node numbers. The mesh size was increased from 1538k to 2243k nodes whilst element size was decreased. There are no significant changes in velocity between nodes 1538k and 1764k. As a result, the succeeding simulations are configured to be more or equal to 1538k nodes. The conventional heating pad arrangement design was chosen for the grid independence test because it has the most complex geometry of all the models in this study. As this model reaches grid independence, the cell size should be successively smaller to reduce error due to discretization while using the same mesh setting as the other models.

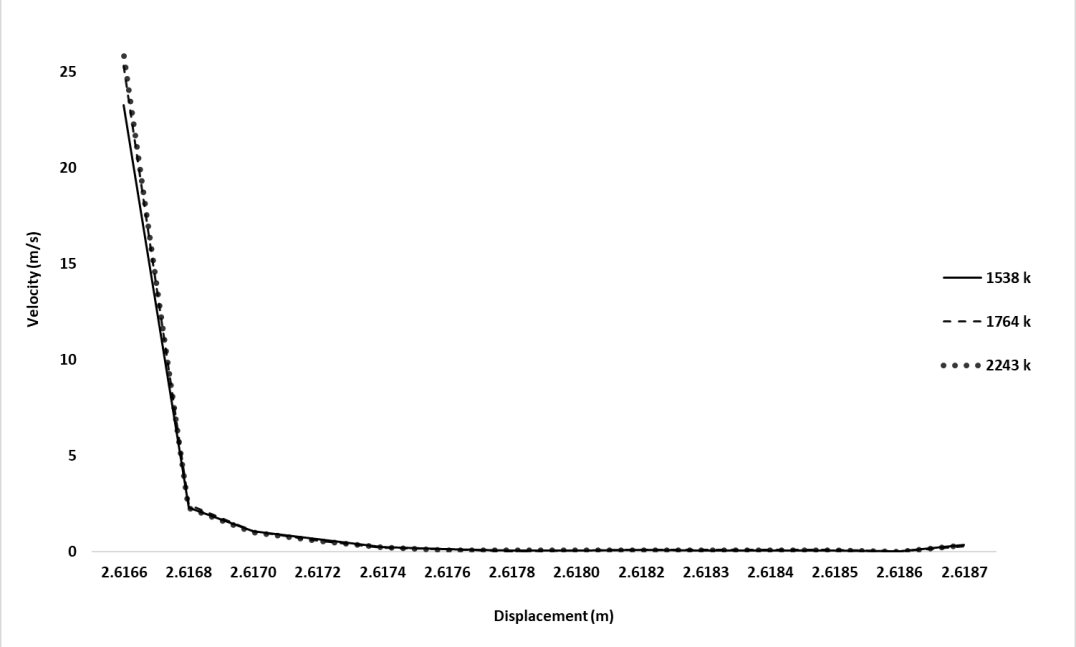

Fig. 5. Grid convergence results of three different nodes

4.2 Validation of Numerical Result

This Figure 6 describes the experimental results compared with the computational result to validate the numerical calculation. This experiment was carried out by indicating four points (inlet 1, inlet 2, outlet 1, and outlet 2), as shown in Figure 3, and the line graph result was based on one of the four points (inlet 1). This experimental data was collected along 30 minutes and was validate with the simulation data for the same duration which is 30 minutes. The induced pressure for the inlet is constantly 1 bar during the experiment and simulation. A data on a line graph represents the temperature rise as time passes. The inlet 1 for experiment and simulation result was slightly

different less than 1%. This shows that this figure verifies the satisfactory agreement between numerical and experimental data. Its confirms that the verified numerical methodology is usable in the future design of heating of floor heating system.

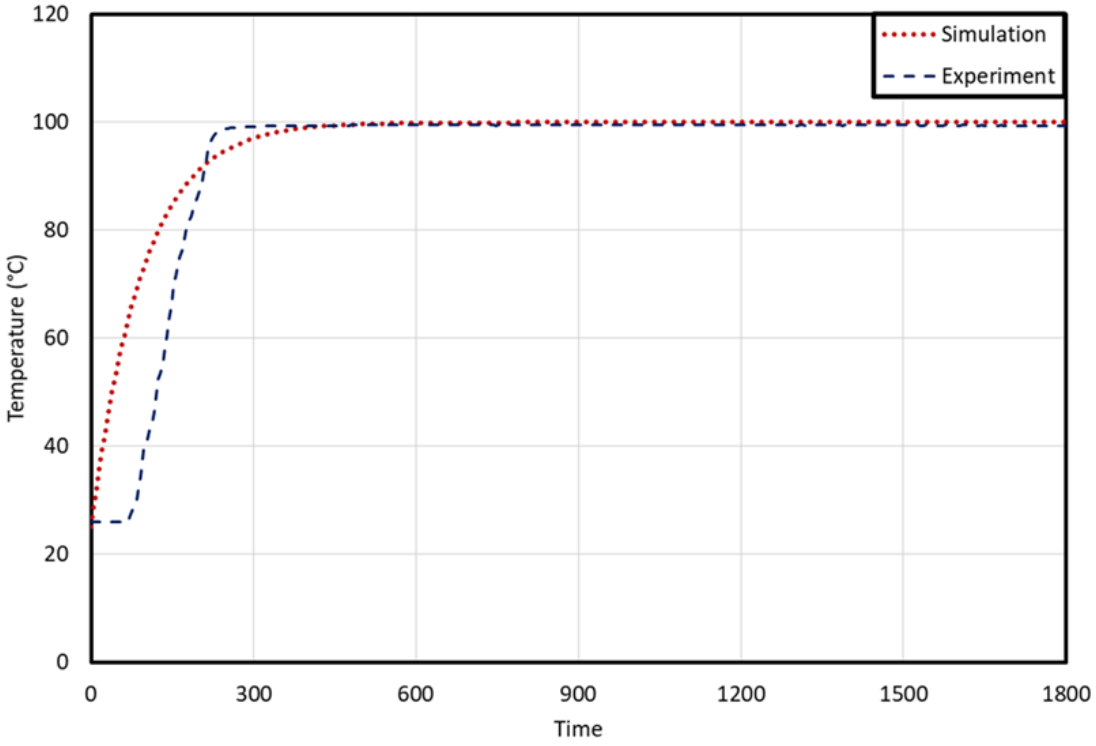

Fig. 6. Validation result of the temperature at point 1 (inlet 1)

4.3 Temperature Distribution of Heating Pad on Different Piping Arrangement

In the floor heating system analysis, the pipe temperature and distribution are the crucial parameters that determine the floor surface temperature and contact wall temperature distribution. Figure 7 showed the temperature distribution contour plots on Z-X plane of heat travels from the inlet to the outlet induced by different pressure inlet. The legend value, which can be seen on the left side, indicates the maximum and minimum values for the contour. The colour contour represents the heating that takes place, the redder the colour of the tube, the greater the heat transfer from the steam. Furthermore, for a better understanding of the contour, Figure 7(a), (b) and (c) was presented. Figure 7(c), which shows a heating pad with a counterflow arrangement, illustrates that when 1bar pressure is created, the maximum heat distribution is clearly visible, but the colour contour caused by 4bar seems dimmer. This situation shows that the slow the heat travels inside the pipe, the higher the heat contact the wall thus, the heat transfer occurred was efficient. Some other obvious temperature distribution clearly can be seen at the serpentine arrangement cases which allocate as Figure 7(b). The different colour obviously can be seen in between 1 to 4 bar pressure induced which the colour is from the reddish to the blueish. This shows that the fundamental theory of Gay Lussac's law which state that the pressure of a given amount of gas held at constant volume is proportional to the temperature [25]. This case was same goes to conventional heating pad arrangement as shown in Figure 7(a). However, the case for conventional heating pad arrangements was differed from the others and didn't obey with the trends. This situation will be taken for further study to determine what is affecting it.

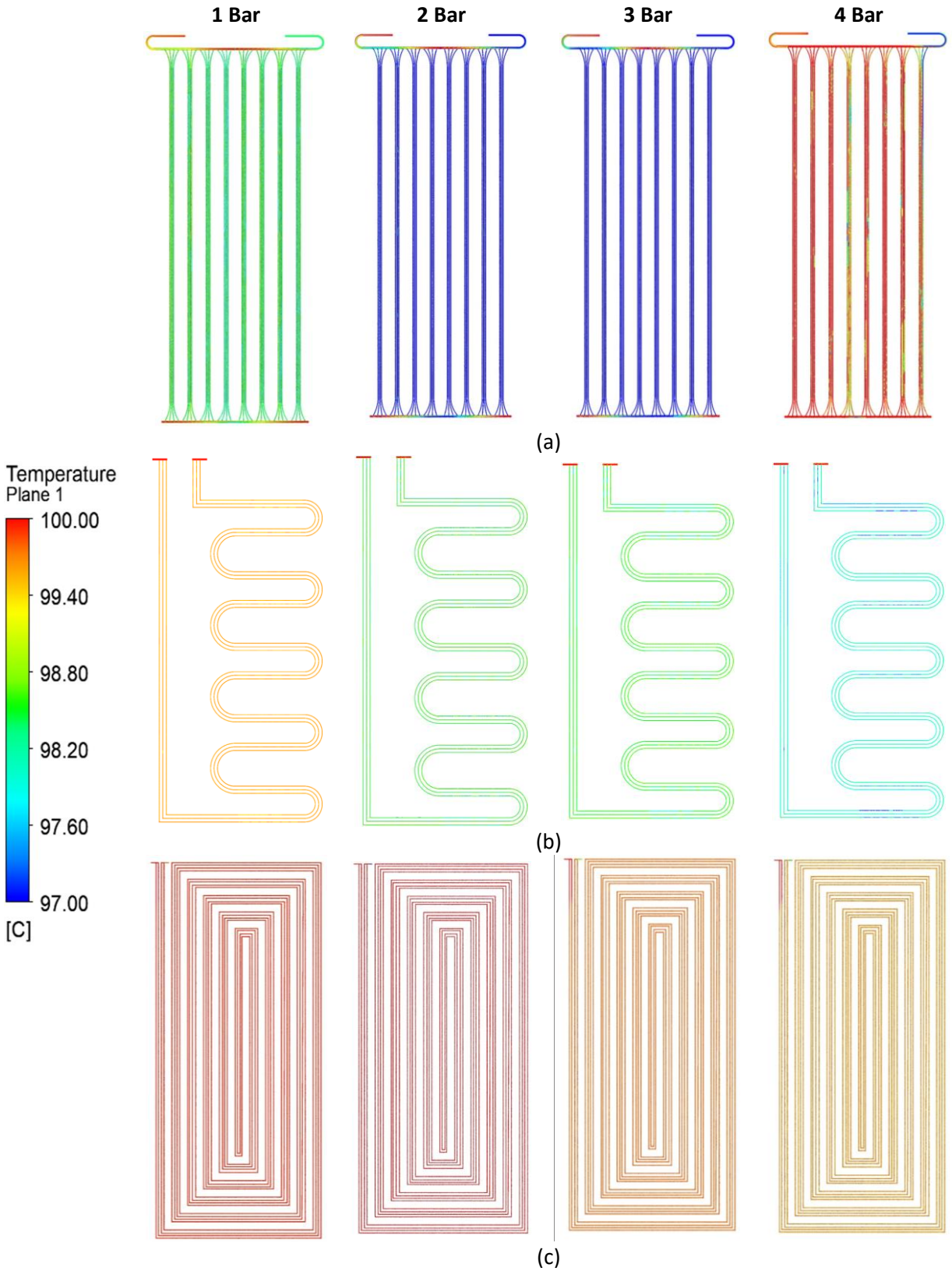

Fig. 7. Temperature Distribution of three different arrangements

4.4 Temperature Distribution Analysis on Flexitank

There is an obvious temperature different from different arrangements of heating pad as shown in Figure 8 by comparing contour profiles. These arrangements generate and heat the bottom surface of flexitank until it reaches the steady state conditions. Some obvious thermal stratification was observed with the colour contour of the flexitank for counterflow arrangement had the higher temperature distribution and uniform, whereas the conventional arrangement had the variety of colour and was the lowest between two other arrangements. According to the previous research between serpentine and counterflow arrangement that had been applied for floor heating system for building application, the counterflow arrangement was better [9, 12, 14]. As a consequence of the numerical calculation, it was demonstrated that this arrangement is also applicable and efficient to be used at the flexitank application. Thus, temperature distribution contour on Figure 8(c) shows the efficiency of heating pad and tendency to heat up the entire flexitank which can reduce the time taken to liquidize the flexitank is better compared to conventional heating pad arrangement.

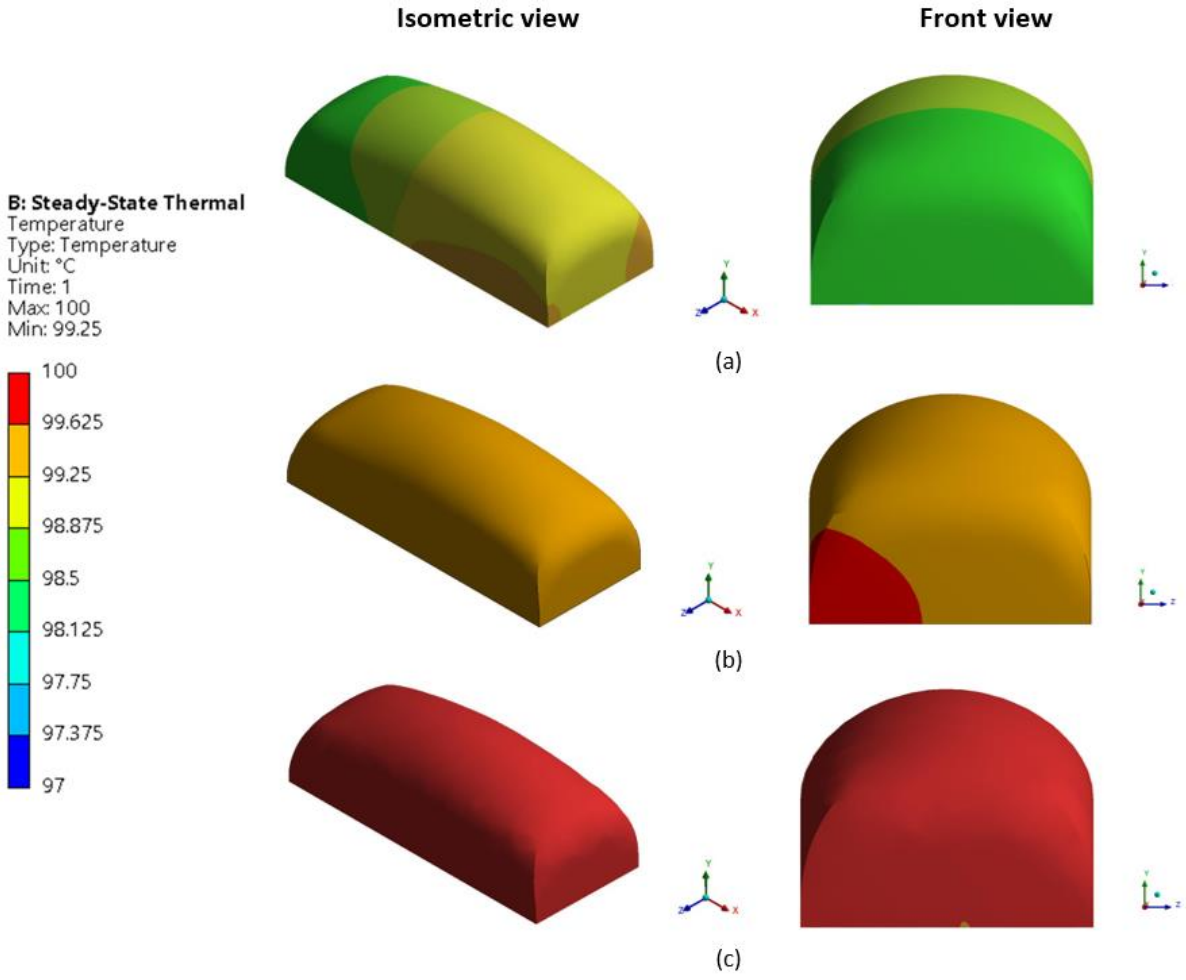

Fig. 8. Temperature Distribution of three different arrangements (a) Conventional arrangement, (b) Serpentine arrangement and (c) Counterflow arrangement on flexitank

4.5 Pressure Distribution Analysis on Heating Pad

Pressure distributions along the heating pad tubes at a steady state condition is shown in Figure 9. It was found that the pressure travels from the inlet to the outlet was higher at the induced

pressure is 4bar. All the pipe arrangements were following the trends. However, from the trends it can be seen that the conventional and serpentine arrangement only covered half of the whole layout while counterflow covered the entire layout.

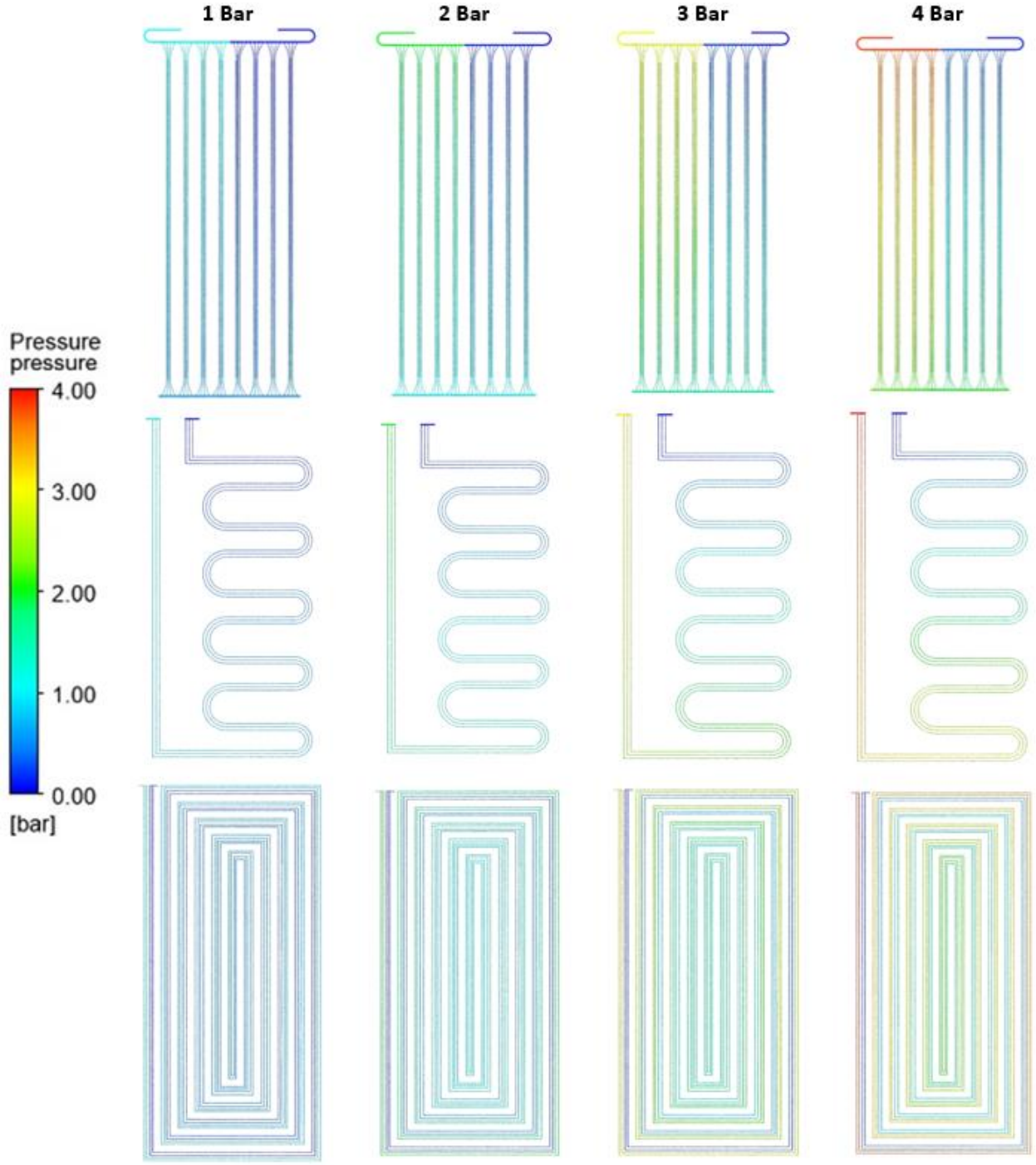

Fig. 9. Pressure Distribution of three different arrangements

4.6 Comparison with Other Studies

Most of the numerical methods applied for this study are nearly similar to that of several other studies [9–13]. However, the study of changes in the pressure inlet on the temperature distribution

and comparing different piping arrangements are different from others. The set of boundary conditions, inlet temperature, inlet parameters, tube spacing, and pipe diameter are different. The study performed a simulation for the same layout by follow the heating pad for 21,000 L flexitank layout and pipe diameter with the same thickness for the different piping arrangements and compared them. This study's significant difference was the temperature distribution for all the cases were simulated in the pipe. The flexitank was consider for a simulation, and the change in temperature field at the flexitank was in the scope. This analysis's basic philosophy is that the uniform temperature distribution in the pipe flow will heat the entire flexitank from the bottom surface.

Among all cases, counterflow arrangement generates the uniform temperature distribution with a minimal temperature gradient of approximately 100◦C. This layout heats the flexitank uniformly and provides better thermal convection between heating pad and flexitank. The worst-case was the conventional arrangement. Most of the region has a temperature below than 97◦C at the flexitank even it was reached the steady state conditions which means the entire flexitank were heated uniformly. The study on the heating pad arrangements were conducted to investigate the temperature distribution and it was similar to them, but the arrangement method and dimensions are different.

4.7 Pressure Losses

Pressure losses are an extremely important factor to consider when constructing heating pad systems because they can have a significant impact on the time it takes for the liquid inside the flexitank to completely liquidise. Thus, total pressure losses were calculated for the three piping layouts and several inlet pressures. Table 4 reassembles the results. As demonstrated in Table 4, an increase in velocity induces an increase in pressure losses for a fixed tubing diameter. Furthermore, minimal pressure losses of 2.486 bar are discovered for the counterflow design. The configuration inducing the higher-pressure losses is the serpentine one.

Table 4
Pressure losses (in bar) for three cases

Piping arrangement	1 Bar	2 Bar	3 Bar	4 Bar
Conventional	0.978 bar	1.953 bar	2.927 bar	0.000 bar
Serpentine	1.000 bar	1.999 bar	2.999 bar	3.998 bar
Counterflow	0.995 bar	1.989 bar	2.983 bar	3.977 bar

5. Conclusion

In this study, CFD simulation of temperature distribution over the heating pad for flexitank applications have been studied for different arrangements with the same specification in terms of material and dimensions. Serpentine arrangement shows the various colour of temperature distribution contour on outer surface of heating pad pipes while uniform contour of reddish was generates by counterflow arrangement which provides better thermal. This situation can be convinced with the result of temperature contour on flexitank which counterflow arrangement heat up the entire flexitank maximumly rather than other arrangements at the steady state conditions.

Therefore, the 1 bar of pressure inlet was chosen as it was enough to heat up the flexitank and it was parallel with the ideal gasses' theory of Gay Lussac's law. Subsequently, further study of thermal distribution can be investigated by using more variable parameters and a wide range of these parameters. Different turbulence models can also be used for conducting a numerical calculation.

Acknowledgment

This research was supported by Industrial Grant (vot M026). The author would like to thank the Faculty of Engineering Technology, Universiti Tun Hussein Onn Malaysia, and MY Flexitank Industries Sdn Bhd for providing necessary research facility for this study.

Reference

[1] "What is Flexitank in Shipping?" https://www.marineinsight.com/maritime-law/what-is-flexitank-in-shipping/ (accessed Jul. 17, 2022).
[2] "Heating Pad - Product Range - Gaoqing Anthente Container Package." https://www.webpackaging.com/en/portals/gaoqinganthentecontainerpackage/assets/11331235/heating-pad/ (accessed Jul. 17, 2022).
[3] "MYFLEXITANK – Your Bulk Liquid Packaging Specialist." https://myflexitank.com/ (accessed Jul. 17, 2022).
[4] Sarbu, Ioan, and Calin Sebarchievici. "A comprehensive review of thermal energy storage." *Sustainability* 10, no. 1 (2018): 191. https://doi.org/10.3390/su10010191
[5] "Heating systems for flexitanks by TRUST Flexitanks." https://www.trustflexitanks.com/productos/flexitank-heating-systems/ (accessed Jul. 17, 2022).
[6] "Heater Pad | SIA Flexitanks | SIA Flexitanks." https://siaflexitanks.com/heater-pad (accessed Jul. 17, 2022).
[7] Damasceno, Flávio A., Carlos EA Oliveira, Jairo AO Saraz, Leonardo Schiassi, and Jofran L. de Oliveira. "Validation of a heating system in the farrowing house using a CFD approach." *Engenharia Agrícola* 38 (2018): 471-477. https://doi.org/10.1590/1809-4430-eng.agric.v38n4p471-477/2018
[8] Lin, Kunping, Yinping Zhang, Xu Xu, Hongfa Di, Rui Yang, and Penghua Qin. "Experimental study of under-floor electric heating system with shape-stabilized PCM plates." *Energy and buildings* 37, no. 3 (2005): 215-220. https://doi.org/10.1016/j.enbuild.2004.06.017
[9] Mishra, Sarika Kumari, Tri Ratna Bajracharya, and Rabindra Nath Bhattarai. "Design and Numerical Analysis of Solar Underfloor Heating System: A Case Study of Resort in Nagarkot, Nepal." In *Proceedings of IOE Graduate Conference*, pp. 529-536. 2017.
[10] Izadi, Mohammad Javad, and Kamyar Makaremi. "Cfd simulation of temperature distribution in a room with various under floor heating system models." In *Fluids Engineering Division Summer Meeting*, vol. 43727, pp. 2319-2329. 2009. https://doi.org/10.1115/FEDSM2009-78545
[11] Wang, Yinghui, Xuelai Zhang, Zhen Tian, and Yuyang Li. "Numerical simulation of thermal performance of indoor airflow in heating room." *Energy Procedia* 158 (2019): 3277-3283. https://doi.org/10.1016/j.egypro.2019.01.983
[12] Aacharya, Ananta, Shuvas Khanal, Bishal Humagain, Sangeet Kattel, and Bivek Baral. "CFD analysis of temperature distribution of different piping arrangement used in radiant floor heating system." *Kathmandu University Journal of Science, Engineering and Technology* 15, no. 2 (2021).
[13] Khorasanizadeh, H., G. A. Sheikhzadeh, A. A. Azemati, and B. Shirkavand Hadavand. "Numerical study of air flow and heat transfer in a two-dimensional enclosure with floor heating." *Energy and buildings* 78 (2014): 98-104. https://doi.org/10.1016/j.enbuild.2014.04.007
[14] Oubenmoh, S., A. Allouhi, A. Ait Mssad, R. Saadani, Tarik Kousksou, M. Rahmoune, and M. Bentaleb. "Some particular design considerations for optimum utilization of under floor heating systems." *Case studies in thermal engineering* 12 (2018): 423-432. https://doi.org/10.1016/j.csite.2018.05.010
[15] Andersson, Bengt, Ronnie Andersson, Love Håkansson, Mikael Mortensen, Rahman Sudiyo, and Berend Van Wachem. *Computational fluid dynamics for engineers*. Cambridge university press, 2011. https://doi.org/10.1017/CBO9781139093590
[16] Japar, Wan Mohd Arif Aziz, Nor Azwadi Che Sidik, Natrah Kamaruzaman, Yutaka Asako, and Nura Mu'az Muhammad. "Hydrothermal performance in the Hydrodynamic Entrance Region of Rectangular Microchannel Heat Sink." *Journal of Advanced Research in Numerical Heat Transfer* 1, no. 1 (2020): 22-31.
[17] Rosli, Mohd Afzanizam Mohd, Irfan Alias Farhan Latif, Muhammad Zaid Nawam, Mohd Noor Asril Saadun, Hasila Jarimi, Mohd Khairul Anuar Sharif, and Sulaiman Ali. "A Simulation Study on Temperature Uniformity of Photovoltaic Thermal Using Computational Fluid Dynamics." *Journal of Advanced Research in Fluid Mechanics and Thermal Sciences* 82, no. 1 (2021): 21-38. https://doi.org/10.37934/arfmts.82.1.2138
[18] Rosli, Mohd Afzanizam Mohd, Yew Wai Loon, Muhammad Zaid Nawam, Suhaimi Misha, Aiman Roslizar, Faridah Hussain, Nurfaizey Abdul Hamid, Zainal Arifin, and Safarudin Gazali Herawan. "Validation Study of Photovoltaic Thermal Nanofluid Based Coolant Using Computational Fluid Dynamics Approach." *CFD Letters* 13, no. 3 (2021): 58-71. https://doi.org/10.37934/cfdl.13.3.5871
[19] Abdullah, Amira Lateef, S. Misha, N. Tamaldin, M. A. M. Rosli, and F. A. Sachit. "Theoretical study and indoor

experimental validation of performance of the new photovoltaic thermal solar collector (PVT) based water system." *Case Studies in Thermal Engineering* 18 (2020): 100595. https://doi.org/10.1016/j.csite.2020.100595

[20] Idris, Muhammad Syafiq, Irnie Azlin Zakaria, and Wan Azmi Wan Hamzah. "Heat transfer and pressure drop of water based hybrid Al2O3: SiO2 nanofluids in cooling plate of PEMFC." *Journal of Advanced Research in Numerical Heat Transfer* 4, no. 1 (2021): 1-13.

[21] Farahani, Somayeh Davoodabadi, Mahdi Alibeigi, and Hamed Hossienabadi Farahani. "The Uniform Magnetic Field Efficacy on Heat Transfer of Nanofluid Flow in A Flat Tube." *Journal of Advanced Research in Numerical Heat Transfer* 5, no. 1 (2021): 9-27.

[22] Rosli, Mohd Afzanizam Mohd, Muhammad Zaid Nawam, Irfan Alias Farhan Latif, Safarudin Ghazali Herawan, Noriffah Md Noh, Siti Nur Dini Noordin Saleem, and Faridah Hussain. "The Effect of Variation in Mass Flow Rate and Solar Irradiance on Temperature Uniformity and Thermal Performance of Photovoltaic Thermal: A Simulated CFD Study." *Journal of Advanced Research in Fluid Mechanics and Thermal Sciences* 91, no. 2 (2022): 106-119. https://doi.org/10.37934/arfmts.91.2.106119

[23] Vestnes, Frida. "A CFD-model of the Fluid Flow in a Hydrogen Peroxide Monopropellant Rocket Engine in ANSYS Fluent 16.2." Master's thesis, NTNU, 2016.

[24] Singh, Lokesh, and A. K. Raghav. "Thermal Performance Investigation of Horizontal Spiral Coiled Tube for Design & Process Parameters Using CFD & DOE Techniques."

[25] "Gay-Lussac's Law: Pressure & Temperature Relationship | Gay-Lussac's Law Equation & Examples - Video & Lesson Transcript | Study.com." https://study.com/academy/lesson/gay-lussacs-law-gas-pressure-and-temperature-relationship.html (accessed Jul. 18, 2022).